RSC Advances

ROYAL SOCIETY OF CHEMISTRY

www.rsc.org/advances

Defect mediated highly enhanced ultraviolet emission in P-doped ZnO nanorods

Sanjit Sarkar and Durga Basak*

Department of Solid State Physics

Indian Association for the Cultivation of Science

Jadavpur, Kolkata-700032

Abstract:

P doped ZnO one-dimensioal (1D) nanorods (NRs) grown by simple hydrothermal method show highly enhanced ultraviolet photoluminescence (UV PL) property as compared to the undoped ZnO sample. A detailed in-depth understanding on the mechanism behind the enhancement has been done by performing experimental analyses on power dependence of and annealing effect on the emissions, low temperature PL (LTPL), and electrical I-V characteristics of various P doped ZnO NR samples. The doped NR samples retain hexagonal wurtzite structure and similar morphology as that of the undoped one. The UV/vis PL intensity ratio becomes 9 for as-grown sample and 22 for annealed 2% P doped sample which is one order higher than that of the undoped ZnO sample. Correlation of the LTPL and electrical I-V characteristics reveals that the high enhancement in the UVPL is due to recombination via shallow acceptor complex defects of P_{Zn}-$2V_{Zn}$ type.

*Corresponding author:

E-mail: sspdb@iacs.res.in

Introduction:

Among all the wide band gap semiconductors, nanostructured ZnO creates a fascinating subject due to its various distinguished applications in electronics, optics and photonics [1-5]. Since, this II-VI technologically important material is environment friendly, abundant and easy to synthesize in one dimensional (1D) form, its nanorods/nanowires (NRs/NWs) structures especially have drawn broad attention of the research community for studying different surface related processes, which are of benefit not only for understanding the fundamental phenomena in low dimensional systems, but also for developing new generation nanodevices with high performance. Tuning the conductivity, gas sensing ability [1], photo-response characteristics [2, 6-8], and room temperature ferromagnetism [4, 9] in 1D ZnO nanostructures has been achieved by doping with various dopants [2, 10-13]. However, besides the goal to be realized, formation of defects by the dopants as well is a commonly occurring problem in ZnO [14]. It often becomes a great concern that it shows a very weak band edge UV emission and/or a comparable visible emission when doped with either n or p-type dopant. This happens especially when facile growth techniques such as hydrothermal or aqueous chemical methods are used for the growth though their versatility [15-16]. Besides an enormous controversies about the origin of the visible emission, it degrades especially the materials' performance for ultraviolet (UV) light emitting diode (LED) applications where both n and p type doping in ZnO is prerequisite. There are several techniques reported to improve the photoluminescence (PL) property of ZnO [6, 17-18], but weak UV emission in doped ZnO mostly remains problematic. Unless, the origin of this weak emission is understood, the luminescence property cannot be improved. There have been very few efforts in this direction. Ahmad et al. [18] have explained that the shallow donor level present in In doped NWs grown by thermal evaporation method is the cause behind the

enhancement of UV PL. While and Ou et al. [17] have also shown enhanced UV emission in N doped ZnO nanoparticles synthesized by laser ablation method. They have assigned the enhancement due to formation of N_O-Zn_i type acceptor. In our previous report, we have demonstrated an enhanced conductivity in Zn doped ZnO NRs grown by hydrothermal method as well as highly enhanced UV emission [19]. We have assigned the origin of the enhanced UV PL to the excess Zn_i in the NRs. P is a commonly used dopant element to synthesize p-type ZnO nanostructures. In this paper, we have demonstrated that P doped ZnO 1D NRs even when grown by simple hydrothermal method, show highly enhanced UV PL property as compared to the undoped ZnO sample. An investigation on the mechanism behind the enhancement has been carried out by performing intricate experimental analyses on power dependence of and annealing effect on emissions, low temperature PL (LTPL), and electrical I-V characteristics of various P doped ZnO NR samples. It is revealed that the enhancement in UVPL is due to the formation of shallow acceptor states of P_{Zn}-$2V_{Zn}$ type complex defects.

Result and discussion:

Formation of highly oriented ZnO along C axis on the glass substrates has been confirmed from the XRD patterns (Fig. 1) which show only (002) peak of hexagonal wurtzite structure (JCPDS: file no. CDF 92 1A APR93). No other P related peak has been observed which an indication of absence of impurity phase is. For doped samples, a small shift in (002) peak position towards the higher 2θ side has been observed from the slow scan of XRD diffraction patterns (the inset in Fig. 1). It shows that the shift occurs till 2% P doping while for 3%, the peak position almost matches with that of ZnO. As the ionic radii of P is much less than that of O (126 pm), a significant change in the c parameter is expected if P substitutes O in ZnO lattice [20] . However this is not the case. The ionic radii of P (58 pm) is lower than that of Zn (74 pm),

which should cause a small shift of (002) peak in higher 2θ if P occupies Zn site. Therefore, our result indicates that P is doped in Zn sites. However, for higher P doping content (3%), the reverse shift indicates that P is no longer occupying the Zn sites.

Further, support of the fact that the undoped and doped ZnO NRs have been grown vertically on the substrate, has been obtained from the FESEM images of the representative samples in Fig. 2. The NRs have a diameter in the range of 40-50 nm and length of ~500 nm irrespective of doping content. Therefore, it is inferred that P doping has not brought any change in the morphology of the NRs.

Presence of P dopant in ZnO NR samples is however confirmed from the XPS measurements. The spectrum of a representative sample in Fig. 3 shows the peaks corresponding to Zn and O. The inset shows the magnified view of the P_{2p} peak of P. The peak position is at 134.7 eV whereas the peak position of the elemental P is ~130 eV. The peak position of P_{2p} at ~135 eV is generally attributed to P-O bonding [21]. In P-doped ZnO, if P sits in Zn site, P-O bonding should be there which should cause a peak at ~135 eV. Therefore the XPS result confirms that P has been incorporated in the ZnO lattice and it sits in the Zn site rather than the O site which is at par with the XRD results.

The PL spectra of all the samples are shown in Fig. 4(a). The spectra show that the undoped ZnO shows a UV emission at 379 nm besides a broad visible emission of comparable intensity. While an appreciable increase in the UV intensity has been taken place, there is only a slight change in the visible emission intensity when doping is done. The UV-to-visible emission (UV/vis) ratio for all the samples has been shown in table I. UV/vis ratio is 1.3 for undoped and becomes 9 for 2% P doped sample. It decreases to 6.6 for 3% P doping. The inset of Fig. 4(a)

shows the magnified view of the UV emissions of the samples. A deep look at the UV emission peak reveals that there is a red shift in the peak position for the doped sample. This is at par with the result obtained by Wang et al. [22] in case of N doped p-type ZnO who have assigned red shift to dominant bound exciton recombination. The highly enhanced UV/vis ratio as well as the shift in the UV peak position suggests us that there is a different recombination mechanism in the doped samples.

To be confirmed about the mechanism of recombination in undoped and doped samples, excitation dependent PL measurements have been done and the plots of integrated intensity with the excitation power for the representative samples have been shown in Fig. 4(b). The value of α is 1.02 for ZnO and 1.18 for 1% P doped samples. The value of α is < 1 for free or free-to-bound recombination and $1< \alpha<2$ for bound exciton recombination [23]. For our ZnO sample, the value of α is very close to 1. Thus the recombinations in undoped ZnO may be dominated by free or free to bound or bound exciton recombination. Tam et al.[24] have also shown that the UV emission in hydrothermally grown ZnO NRs is dominated by donor bound excitonic recombination from LTPL experiments. They however did not say anything on power dependence. While in our earlier report [19], we too have shown an ultra high UV luminescence in ZnO NRs (grown in excess Zn environment) due to an enhanced free hole to neutral donor bound (h, D) recombination causing value of $\alpha = 0.94$. While for the doped ZnO, the super linear relation between integrated PL intensity and excitation power reflects that the recombination is dominated by bound recombination [23]. Hwang et al. [25] and Xiu et al. [26] have observed that the acceptor bound recombination dominates in the UV emission of P doped ZnO thin film. Therefore, from the experimental observations and concurrence with the earlier reports, it may

be inferred at this stage that the UV emission is most likely dominated by the acceptor bound recombination in P-doped ZnO samples.

To confirm the recombination process, LTPL measurement has been performed for undoped and doped ZnO samples Fig. 5(a & b). The undoped ZnO NRs shows three peaks in the UV region at 3.363, 3.233 and 3.11 eV which correspond respectively to recombination of a neutral donor bound exciton (D^0X), donor-to-acceptor pair transition (DAP) and longitudinal optical phonon replica of the DAP [6, 21]. On the other hand, the PL spectrum of P doped ZnO consists of three peaks at 3.355, 3.315 and 3.235 eV which correspond respectively to recombination of neutral acceptor bound exciton, free-to-neutral acceptor transition and donor acceptor pair recombinations [6, 21, 27-28]. The spectrum is dominated by acceptor bound recombination as observed by Xiu et al. [26]. As the XPS spectrum indicates that P sits on the Zn site, it is most likely that P_{Zn} type of defects have been formed instead of P_O where P_{Zn} acts as a donor [29]. The acceptor energy of P doped ZnO can be calculated by taking the energy of FA transition as 3.315 eV (Fig. 5(a&b)) and band gap as 3.437 eV [25] using the equation, $E_{FA} = E_g - E_A + kT/2$ where E_g and E_A are band gap and acceptor energy [21]. At 10 K temperature, we may neglect kT/2 term and the acceptor energy, E_A is found to be 122 meV, which is in well agreement with the acceptor energy value of P_{Zn}-$2V_{Zn}$ type complex defects [21, 29]. Therefore, the acceptor level in our P doped samples may be assigned to P_{Zn}-$2V_{Zn}$ defects.

It is expected that some point defects should be annealed out upon heating that would give rise to a different emission characteristics. Thus, in order to have more information about defect related recombinations, the samples have been annealed at three different temperatures higher than the growth temperatures. The PL spectra of the annealed samples have been shown in Fig. 5(c&d) and the values of UV/vis ratio calculated from the figure are shown in table I. All

the samples except 3PZnO show a highly enhanced UV/vis ratio due to 250 ^{0}C annealing. The UV/vis ratio becomes 22 for 2PZnO sample which is one order higher than that of undoped ZnO sample. This result is at par with the results obtained by Djurisic et al. [30]. The enhancement in the UV/vis ratio in hydrothermally grown ZnO sample is due to desorption of hydroxyl groups and hydroxides from NRs surface [30]. Desorption of hydroxyl groups start at as low as 150 ^{0}C. The UV/vis ratio of all the samples becomes nearly equal after annealing at 500 ^{0}C. This indicates that the defects responsible for the enhancement of UV/vis ratio in doped sample have been annealed out at 500 ^{0}C. Tam et al. [24] have explained that V_{Zn} and its complex form is annealed out at a temperature ~550 K. Tuomisto et al. [31] also have observed that V_{Zn} and its complexes are annealed out at the temperature range 300–600 K. Djurisic et al. [30] described that the removal of hydrogen related defects also worsen the UV emission in ZnO nanostructures. It may be noticed that drop in UV/Vis ratio for the doped sample is much more than the undoped NRs after 500 ^{0}C annealing. Therefore, it may be concluded that in the doped samples, dominating V_{Zn} related acceptor defects becomes mobile and annealed out at temperature 500 ^{0}C.

The presence of acceptor type defects in the doped samples is further confirmed by the I-V measurement as shown in Fig. 6. The dark current fall by an order for 1PZnO sample and increases for higher concentration of P. Undoped ZnO is intrinsically n type material. For lightly p type doping, acceptors are probably formed which are being compensated resulting a decrease in the dark current [2, 32]. With further increase in doping concentration, an increase in the dark current may be due to the presence of uncompensated P_{Zn} type of defects which act as donor, thus increasing the dark current. The I-V measurement of the annealed samples shows that the dark current of 1PZnO and 2PZnO become much higher compared to that of the undoped

sample. V_{Zn} defects are expected to be annealed out due to annealing at 500 ^{0}C and probability of P_{Zn} in the lattice increases which should increase the conductivity. Therefore, a decreased dark current in as-grown and an increased dark current after annealing ensure formation of P_{Zn}-V_{Zn} acceptor defects in ZnO NRs. This further confirms that the mechanism behind the enhanced UVPL in P doped ZnO is acceptor bound recombination. The schematic in Fig. 6(c) shows the probable defect mediated recombination pathway in P doped ZnO NRs.

Experimental:

P doped ZnO NRs' array has been grown on glass substrate by simple hydrothermal method. First of all, a ZnO seed layer was deposited on ultra-sonically cleaned ordinary glass substrate by RF sputtering method. The details of the seed layer deposition process have been described elsewhere [19]. 10 mM zinc acetate and 10 mM hexamethylene tetramine (HMT) were dissolved in 40 ml of deionized water and kept under constant stirring. 1 mM CTAB has been added to the solution and stirred for 40 minutes. Then the solution had been transferred to a 60 ml Teflon lined stainless steel autoclave and the pre-seeded substrates were placed. Next, the autoclave was kept in an oven preheated at 100 ^{0}C for 20 hours. After the reaction was over, the autoclave was cooled down to room temperature and the substrate was washed and dried at 90^{0}C for further characterization. For doped NRs, firstly, 10 mM zinc acetate was dissolved in 40 ml deionized water and then calculated amount of ammonium dihydrogen phosphate was added to the solution so as to maintain 1, 2 and 3 atomic % P concentration in the precursor solution. For simplicity, the samples grown with 0, 1, 2 and 3 atomic % P in precursor solutions have been named as 0PZnO, 1PZnO, 2PZnO and 3PZnO respectively.

The structural and morphological confirmation were done by using X-ray diffractometer (Bruker, model D8) and field emission electron microscope (JEOL, model JEM2010). The room temperature PL was measured using a He-Cd laser as 325 nm excitation source (Kimmon Koha Co., Ltd.; Model KR1801C) of excitation power 100 mW, a spectrometer and a photomultiplier tube (Horiba Jobin Yvon, Model: iHR 320). X-ray photoelectron spectroscopy (XPS) was done by Omicron XPS instrument (Serial no. 0571). For I-V measurements two gold electrodes were thermally evaporated through a shadow mask at a separation of 3 mm with a diameter of 1 mm on the top of ZnO NRs' array. The currents were measured under a certain bias voltage using a Keithley source meter (model 2400).

Conclusion:

In summary, highly enhanced UV/vis ratio in P doped ZnO NRs grown by low temperature hydrothermal method has been demonstrated. The mechanism behind this enhancement has been established as P_{Zn}-$2V_{Zn}$ type acceptor defect mediated recombination from the support of power dependence of and annealing effect on emissions, LTPL, and I-V measurements. This study will be beneficial for understanding and designing highly emissive p-type ZnO nanostructures for LED applications.

Acknowledgement:

The authors thank CSIR for funding the work vide project no: 03(1260)/12/EMR-II. One of the authors Mr. Sanjit Sarkar acknowledges CSIR, Delhi for providing the fellowship.

References:

1. C. S. Rout, A. R. Raju, A. Govindaraj, C. N. R. Rao, *J. Nanosci. Nanotechnol.* 2007, **7,** 1923-1929.

2. S. Sarkar, D. Basak, *App. Phys. Lett.* 2013, **103,** 041112.

3. K. R. Kittilstved, D. R. Gamelin, *J. Am.Chem. Soc.* 2005, **127,** 5292-5293.

4. P. Sharma, A. Gupta, K. V. Rao, F. J. Owens, R. Sharma, R. Ahuja, J. M. O. Guillen, B. Johansson, G. A. Gehring, *Nat. Mater.* 2003, **2,** 673-677.

5. M. Pal, S. Bera, S. Sarkar, S. Jana, *RSC Adv.* 2014, **4,** 11552-11563.

6. P. J. Li, Z. M. Liao, X. Z. Zhang, X. J. Zhang, H. C. Zhu, J. Y. Gao, K. Laurent, Y. Leprince-Wang, N. Wang, D. P. Yu, *Nano Lett.* 2009, **9,** 2513-2518.

7. D. L. Shao, M. P. Yu, H. T. Sun, T. Hu, J. Lian, S. Sawyer, *Nanoscale* 2013, **5,** 3664-3667.

8. D. L. Shao, M. P. Yu, J. Lian, S. Sawyer, *Appl. Phys. Lett.* 2012, **101,** 211103.

9. Y. F. Li, R. Deng, Y. F. Tian, B. Yao, T. Wu, *Appl. Phys. Lett.* 2012, **100**.

10. H. Y. Peng, G. P. Li, J. Y. Ye, Z. P. Wei, Z. Zhang, D. D. Wang, G. Z. Xing, T. Wu, *Appl. Phys. Lett.* 2010, **96,** 192113.

11. Y. F. Tian, Y. F. Li, T. Wu, *Appl. Phys. Lett.* 2011, **99,** 222503.

12. S. Y. Park, B. J. Kim, K. Kim, M. S. Kang, K. H. Lim, T. Il Lee, J. M. Myoung, H. K. Baik, J. H. Cho, Y. S. Kim, *Adv. Mater.* 2012, **24,** 834-+.

13. K. Mahmood, R. Munir, B. S. Swain, G. S. Han, B. J. Kim, H. S. Jung, *RSC Adv.* 2014, **4,** 9072-9077.

14. A. George, S. K. Sharma, S. Chawla, M. M. Malik, M. S. Qureshi, *J. Alloy. Compd.* 2011, **509,** 5942-5946.

15. H. Ago, Y. Ito, N. Mizuta, K. Yoshida, B. Hu, C. M. Orofeo, M. Tsuji, K. Ikeda, S. Mizuno, 2010, **4,** 7407-7414.

16. X. H. Huang, C. Zhang, C. B. Tay, T. Venkatesan, S. J. Chua, *Appl. Phys. Lett.* 2013, **102,** 111106.

17. Q. Ou, K. Shinji, A. Ogino, M. Nagatsu, *J. Phys. D. Appl. Phys.* 2008, **41,** 205104.

18. M. Ahmad, H. Y. Sun, J. Zhu, *ACS Appl. Mater. Interfaces* 2011, **3,** 1299-1305.

19. S. Sarkar, D. Basak, *Chem. Phys. Lett.* 2011, **516,** 192-198.

20. J. Karamdel, C. F. Dee, K. G. Saw, B. Varghese, C. H. Sow, I. Ahmad, B. Y. Majlis, *J. Alloy. Compd.* 2012, **512,** 68-72.

21. X. H. Pan, J. Jiang, Y. J. Zeng, H. P. He, L. P. Zhu, Z. Z. Ye, B. H. Zhao, X. Q. Pan, *J. Appl. Phys.* 2008, **103,** 023708.

22. X. Q. Wang, S. R. Yang, J. Z. Wang, M. T. Li, X. Y. Jiang, G. T. Du, X. Liu, R. P. H. Chang, *J. Cryst. Growth.* 2001, **226,** 123-129.

23. V. A. Fonoberov, K. A. Alim, A. A. Balandin, F. X. Xiu, J. L. Liu, *Phys. Rev. B* 2006, **73,** 165317.

24. K. H. Tam, C. K. Cheung, Y. H. Leung, A. B. Djurisic, C. C. Ling, C. D. Beling, S. Fung, W. M. Kwok, W. K. Chan, D. L. Phillips, L. Ding, W. K. Ge, *J. Phys. Chem. B* 2006, **110,** 20865-20871.

25. D. K. Hwang, H. S. Kim, J. H. Lim, J. Y. Oh, J. H. Yang, S. J. Park, K. K. Kim, D. C. Look, Y. S. Park, *Appl. Phys. Lett.* 2005, **86,** 151917.

26. F. X. Xiu, Z. Yang, L. J. Mandalapu, J. L. Liu, W. P. Beyermann, *Appl. Phys. Lett.* 2006, **88,** 052106

27. K. K. Kim, H. S. Kim, D. K. Hwang, J. H. Lim, S. J. Park, *Appl. Phys. Lett.* 2003, **83,** 63-65.

28. B. Q. Cao, M. Lorenz, A. Rahm, H. von Wenckstern, C. Czekalla, J. Lenzner, G. Benndorf, M. Grundmann, *Nanotechnology* 2007, **18,** 455707.

29. W. J. Lee, J. Kang, K. J. Chang, *Phys. Rev. B* 2006, **73,** 024117.

30. A. B. Djurisic, Y. H. Leung, K. H. Tam, Y. F. Hsu, L. Ding, W. K. Ge, Y. C. Zhong, K. S. Wong, W. K. Chan, H. L. Tam, K. W. Cheah, W. M. Kwok, D. L. Phillips, *Nanotechnology* 2007, **18,** 095702.

31. F. Tuomisto, K. Saarinen, D. C. Look, G. C. Farlow, *Phys. Rev. B* 2005, **72,** 085206.

32. T. Ghosh, M. Dutta, S. Mridha, D. Basak, *J. Electrochem. Soc.* 2009, **156,** H285-H289.

Table I: The VU/ vis ratios of as grown and annealed samples

Sample name	UV/vis ratio		
	As grown	Annealed at 250^0C	Annealed at 500^0C
ZnO	1.3	2.0	0.46
1PZnO	7.2	16.4	0.75
2PZnO	9.0	22.0	0.76
3PZnO	6.6	4.76	0.46

Figure Captions:

Fig. 1: (a) XRD pattern of the undoped and doped ZnO NRs. Inset shows the slow scan of (002) peak of the samples.

Fig. 2: FESEM images of representative ZnO NRs (a) undoped and (b) 1% P doped ZnO NRs. (c) and (d) are the cross-sectional view of undoped and 1% P doped ZnO NRs respectively.

Fig. 3: XPS spectrum of the doped ZnO NRs. Inset shows the magnified view of P peak.

Fig. 4: (a) Room temperature PL spectra of the undoped and doped ZnO NRs. Inset shows the magnified view of the UV peaks. (b) Excitation power dependent PL of the representative undoped and doped ZnO NRs.

Fig. 5: Low temperature PL spectrum of (a) undoped and (b) 1% P doped ZnO NRs. Room temperature PL spectra of the annealed NRs at (c) 250 ^{0}C and (d) 500 ^{0}C temperatures.

Fig. 6: I-V characteristics of ZnO NRs (a) as-grown and (b) annealed at 500 ^{0}C. (c) The schematic showing possible recombination pathway in P doped ZnO NR.

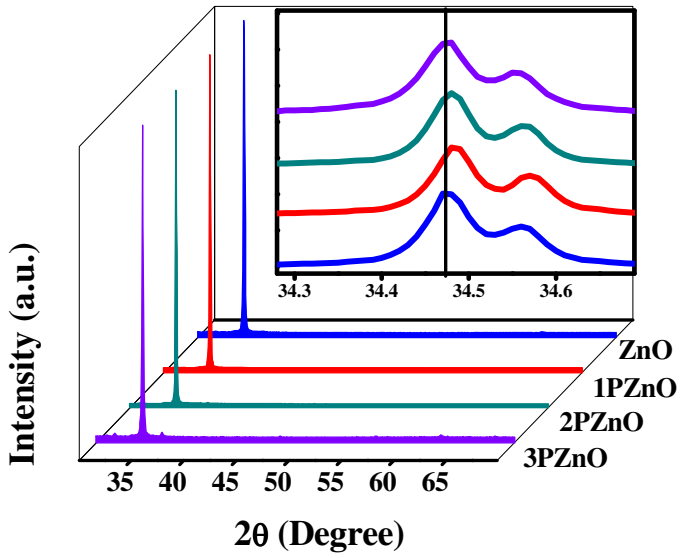

Fig. 1

Sarkar et al.

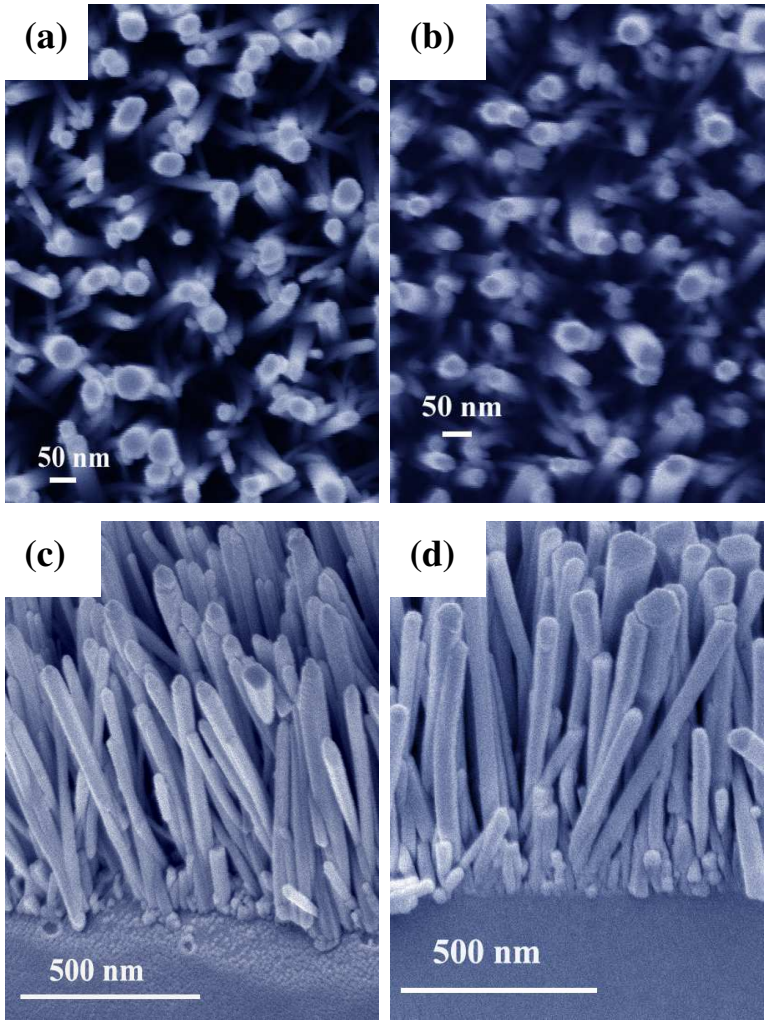

Fig. 2

Sarkar et al.

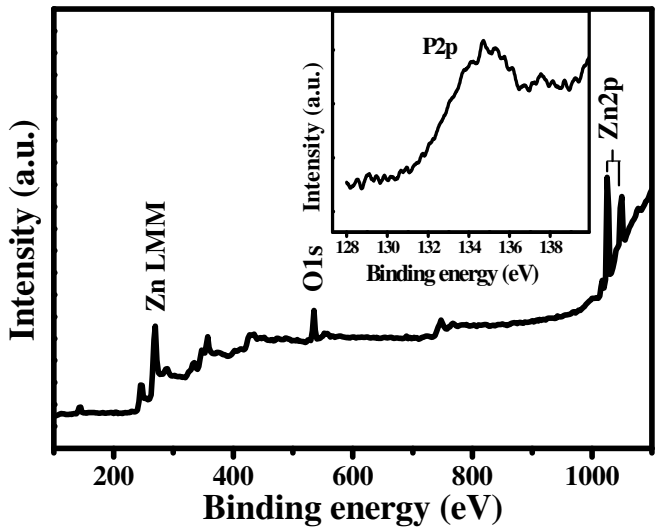

Fig. 3

Sarkar et al.

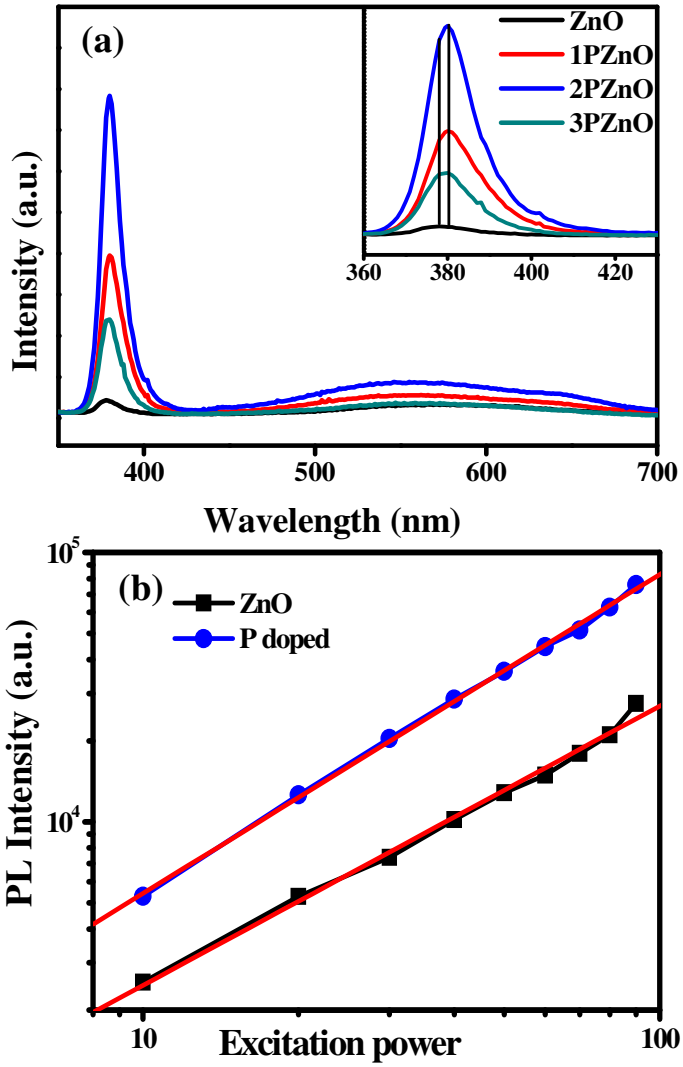

Fig. 4

Sarkar et al.

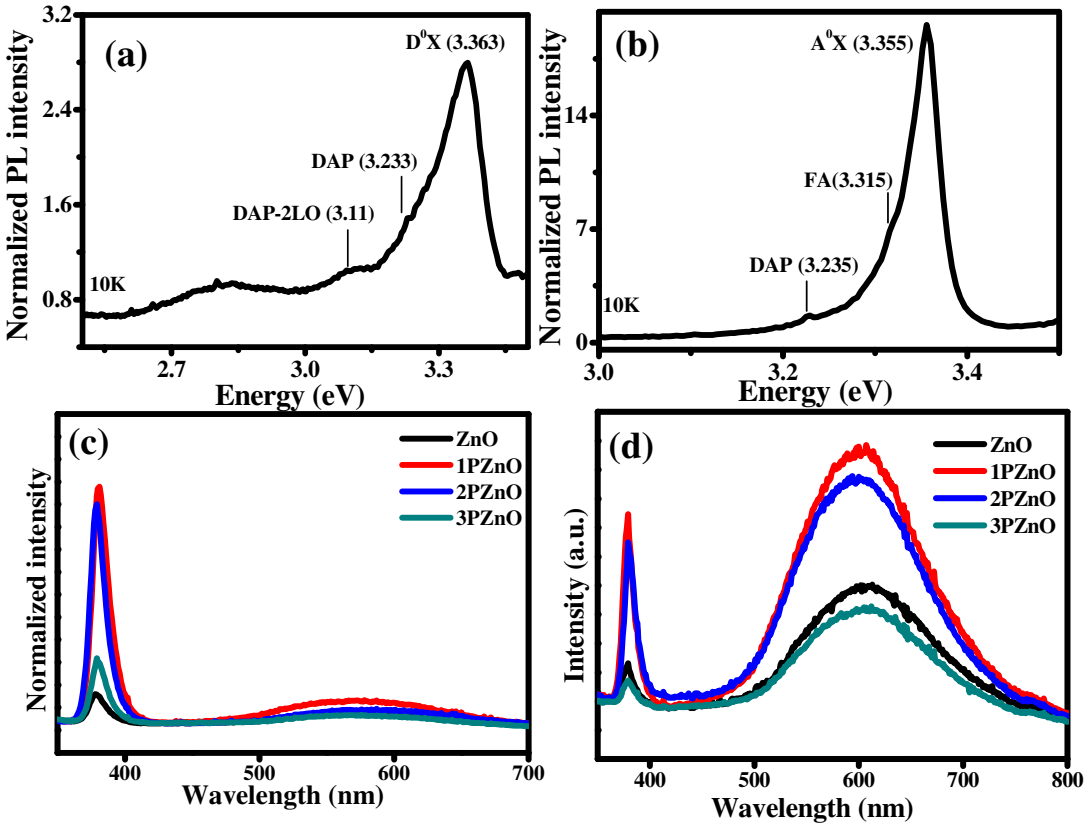

Fig. 5

Sarkar et al.

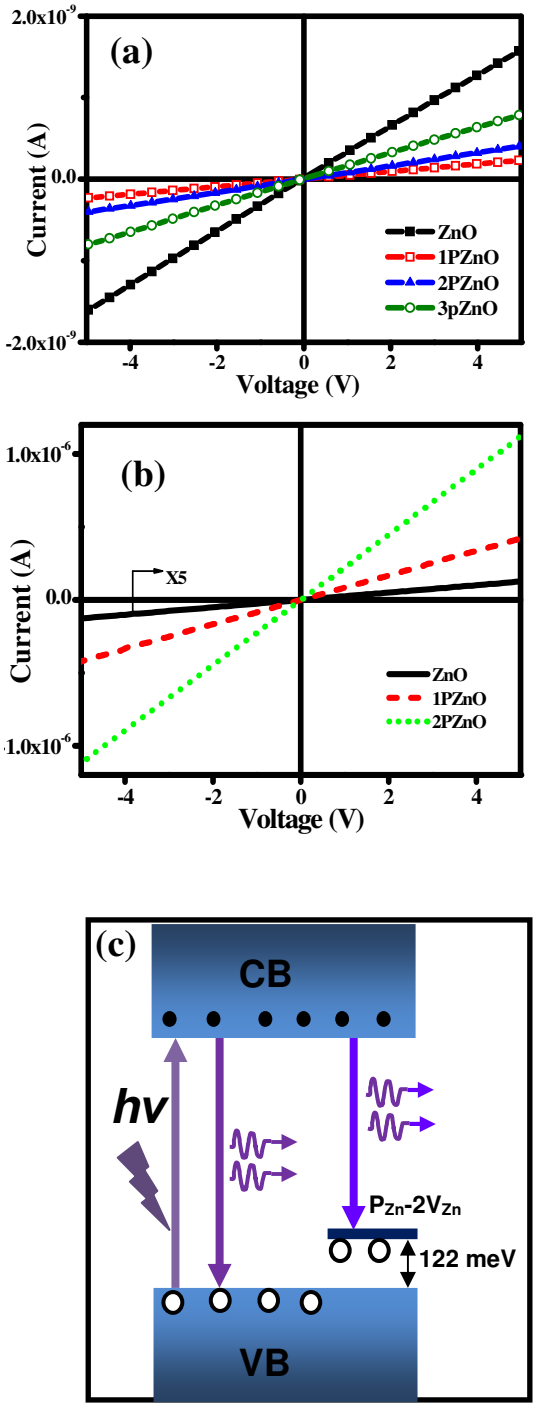

Fig. 6

Sarkar et al.